Bulletin of the Seismological Society of America. Vol. 65, No. 5, pp. 1073–1095. October 1975

THEORETICAL BASIS OF SOME EMPIRICAL RELATIONS IN SEISMOLOGY

BY HIROO KANAMORI AND DON L. ANDERSON

ABSTRACT

Empirical relations involving seismic moment M_o, magnitude M_S, energy E_S and fault dimension L (or area S) are discussed on the basis of an extensive set of earthquake data ($M_S \geqq 6$) and simple crack and dynamic dislocation models. The relation between log S and log M_o is remarkably linear (slope $\sim 2/3$) indicating a constant stress drop $\Delta\sigma$; $\Delta\sigma = 30$, 100 and 60 bars are obtained for inter-plate, intra-plate and "average" earthquakes, respectively. Except for very large earthquakes, the relation $M_S \sim (2/3) \log M_o \sim 2 \log L$ is established by the data. This is consistent with the dynamic dislocation model for point dislocation rise times and rupture times of most earthquakes. For very large earthquakes $M_S \sim (1/3) \log M_o \sim \log L \sim (1/3) \log E_S$. For very small earthquakes $M_S \sim \log M_o \sim 3 \log L \sim \log E_S$. Scaling rules are assumed and justified. This model predicts $\log E_S \sim 1.5 M_S \sim 3 \log L$ which is consistent with the Gutenberg-Richter relation. Since the static energy is proportional to $\bar{\sigma} L^3$, where $\bar{\sigma}$ is the average stress, this relation suggests a constant apparent stress $\eta\bar{\sigma}$ where η is the efficiency. The earthquake data suggest $\eta\bar{\sigma} \sim \frac{1}{2}\Delta\sigma$. These relations lead to $\log S \sim M_S$ consistent with the empirical relation. This relation together with a simple geometrical argument explains the magnitude-frequency relation $\log N \sim -M_S$.

INTRODUCTION

The magnitude was the first quantitative measure of the strength of an earthquake. It is still the most widely used earthquake parameter although its shortcomings are well known. It is also the most difficult parameter to relate theoretically to other important source characteristics such as strain energy release, fault offset, stress drop, source dimension, moment and radiated seismic energy. These other parameters can be related, one to another, fairly easily, but their relationship to magnitude requires a spectral description of the seismic source. Such a description requires a complete time and space history of the faulting or stress release mechanism. For example, the magnitude is calculated from seismic-wave amplitudes at a given period while the seismic energy release involves integration over the whole spectrum. The seismic moment is determined from the long-period level which may be quite removed, in period or frequency, from the period at which the magnitude is measured. In the first part of this paper, we summarize the relationships among the fault parameters which can be derived from static crack or dislocation theories. We then use dynamic theories of the faulting process to relate magnitudes to these other source parameters. In particular, we derive a general relationship between magnitude and radiated seismic energy. We derive the Gutenberg-Richter energy magnitude relation $\log E_S \sim 1.5 M_S$ and demonstrate under what conditions it is valid. In the process, we show the relationship between magnitude, fault dimension, stress drop, and moment. These relationships depend on such dimensionless parameters as the ratio of rise time to total fracture time or ratios involving the coherence length, coherence time, and local rupture velocity. In going from static models to seismic measurements, param-

eters such as efficiency, stress drop, and mean stress are also important. We will show that very simple crack and dynamic dislocation models can explain various important empirical relations observed for large ($M_S \geqq 6.0$) earthquakes for which the observed data are most accurate and complete.

Source Parameters

From the static or geological point of view the important faulting parameters are dimension, $\tilde{L}$, and average offset, $\bar{D}$. From these, and the material properties μ (or λ and μ) the static moment, M_o, can be calculated. The mean stress, $\bar{\sigma}$, also is required to calculate the strain energy change, ΔW, associated with faulting. Some fraction, η, of this is available for radiation as seismic energy. Three independent source parameters are therefore required to describe the statics of faulting; $\tilde{L}$, $\bar{D}$, and $\bar{\sigma}$ or $\tilde{L}$, M_o, and ΔW, for example. A parameter often used in discussions of fault mechanisms is the stress drop, $\Delta\sigma$. This however, is simply $\mu\bar{D}/\tilde{L}$.

A seismogram contains information relevant to all of the above parameters but to be interpreted must be corrected for distortion by the instrument and the Earth and for dynamic properties of the source such as rise time (τ) and duration (t_c) and direction of faulting. Although in some cases the rise time, or source-time function, can be determined from the seismogram, the information usually available is the amplitude at some frequency (the magnitude). The total energy contained in the seismogram and the long-period level (the seismic moment) can be obtained from special studies using appropriate instruments. If all earthquakes are "similar", a measurement of amplitude at a single frequency defines the spectrum, and scaling laws such as those proposed by Aki (1967) can be used to estimate the other parameters such as moment and energy. This kind of scaling, in fact, is implicit in attempts to relate magnitude to energy (Gutenberg and Richter, 1956) or moment (Brune and Engen, 1969; Aki, 1967).

In this paper the independent source parameters used most often will be S (fault area $\sim \tilde{L}^2$), $\Delta\sigma$ (stress drop), $\eta\bar{\sigma}$ (apparent stress), E_S (seismic energy), M_o (moment), τ (rise time), and t_c (duration of faulting $= \tilde{L}/v$ where v is average propagation velocity). Assumptions of similarity and scaling and spectral source theories can be used to interrelate some of these parameters and to involve M_S (magnitude) in the discussion.

Static Theories

Figure 1 summarizes the relationships between average offset, $\bar{D}$, stress drop, $\Delta\sigma$, and strain energy, ΔW, for circular faults (Eshelby, 1957; Keilis Borok, 1959), strike-slip faults (Knopoff, 1958) and dip-slip faults (Starr, 1928). The dimensions of the fault are a (radius) or L and w (length and width) which we represent by $\tilde{L}$. For a vertical fault w is the depth interval over which displacement occurs. The mean stress, $\bar{\sigma}$, and stress drop, $\Delta\sigma$, are $(\sigma_0+\sigma_1)/2$ and $\sigma_0-\sigma_1$, respectively, where σ_0 is the initial stress and σ_1 the final stress.

The stress drop $\Delta\sigma$ is given by

$$\Delta\sigma = C\mu(\bar{D}/\tilde{L}) \tag{1}$$

where μ is the rigidity, and C is a nondimensional shape factor. $\bar{D}/\tilde{L} \equiv \Delta\tilde{e}$ is the representative strain change, or strain drop. For circular faults $\tilde{L} = a$ and $C = 7\pi/16$ (Eshelby, 1957; Keilis Borok, 1959). For shallow infinite longitudinal shear faults (strike slip), $\tilde{L} = w$ and $C = 2/\pi$ (Knopoff, 1958). For shallow infinite transverse shear faults (dip

slip), $\tilde{L} = w$ and $C = 4(\lambda+\mu)/\pi(\lambda+2\mu)$ where λ is the Lamé constant (Starr, 1928; Aki, 1966). In all cases $C \approx 1$. In the latter two cases the free surface effect is included (Knopoff, 1958; Aki, 1966). For a finite rectangular fault of length L, relation (1) holds only approximately, but it is a reasonably good approximation (Chinnery, 1964; Sato, 1972). The change in the strain energy ΔW is given by

$$\Delta W = S\bar{D}\bar{\sigma} = (\tilde{L}/C\mu)S\Delta\sigma\bar{\sigma} = (\tilde{L}/2C\mu)S(\sigma_0{}^2 - \sigma_1{}^2) \tag{2}$$

where S is the fault area.

The static moment M_o is

$$M_o = \mu S\bar{D} = (\tilde{L}/C)S\Delta\sigma = (\mu/\bar{\sigma})\Delta W.$$

The radiated seismic energy E_S is

$$E_S = \eta\Delta W$$

where η is the seismic efficiency of $\eta < 1$.

	Circular ($\lambda = \mu$)	Strike Slip	Dip Slip
Stress drop ($\Delta\sigma$)	$\frac{7\pi}{16}\mu\frac{(\bar{D})}{a}$	$\frac{2}{\pi}\mu\left(\frac{\bar{D}}{w}\right)$	$\frac{4(\lambda+\mu)}{\pi(\lambda+2\mu)}\mu\left(\frac{\bar{D}}{w}\right)$
Strain energy ($\Delta W = S\sigma D$)	$\frac{16}{7\mu}a^3\Delta\sigma\bar{\sigma}$	$\frac{\pi}{2\mu}w^2L\Delta\sigma\bar{\sigma}$	$\frac{\pi(\lambda+2\mu)}{4(\lambda+\mu)\mu}w^2L\Delta\sigma\bar{\sigma}$
Moment ($M_o = \mu S\bar{D}$)	$\frac{16}{7}\Delta\sigma a^3$	$\frac{\pi}{2}\Delta\sigma w^2L$	$\frac{\pi(\lambda+2\mu)}{4(\lambda+\mu)}\Delta\sigma w^2L$

FIG. 1. Relations between stress drop, strain energy, offset, dimension, and moment for static cracks. Dimensions of the fault are a radius, L length, w width; initial stress is σ_0; final stress is σ_1; stress drop is $\Delta\sigma = \sigma_0 - \sigma_1$; average stress is $\bar{\sigma} = (\sigma_0+\sigma_1)/2$; average dislocation is $\bar{D}$.

DYNAMIC THEORIES

Consider a unilateral propagating fault of length L, width w, and area wL. The dislocation time function is assumed to be a linear ramp function of rise time τ. Then, the amplitude spectral density $|\hat{u}_c(\omega)|$ of the far-field displacement in an infinite homogeneous medium resulting from this source is given by (Haskell, 1964),

$$\left|\hat{u}_c(\omega)\right| = \frac{\mu\bar{D}Lw}{4\pi\rho r u_c{}^3} R^c_{\theta\phi}\left|\frac{\sin\frac{\omega\tau}{2}}{\frac{\omega\tau}{2}}\right|\left|\frac{\sin\frac{\omega t_c}{2}}{\frac{\omega t_c}{2}}\right| \tag{3}$$

where $\bar{D}$ is the dislocation (offset), ρ the density, r the distance, u_c the wave velocity, either P or S velocity, and $R^c_{\theta\phi}$ represents the radiation pattern (for notation see Haskell, 1964). t_c is the rupture-time constant given by

$$t_c = L/u - (L/u_c)\cos\Theta$$

where Θ is the azimuth of the station measured from the rupture direction.

Aki's (1967) statistical model replaces τ and L by two statistical parameters, correlation time k_T^{-1} and correlation length k_L^{-1}. The function

$$\left|\frac{\sin\frac{\omega\tau}{2}}{\frac{\omega\tau}{2}}\right|\left|\frac{\sin\frac{\omega t_c}{2}}{\frac{\omega t_c}{2}}\right|$$

is replaced by

$$\left\{1+\left(\frac{\omega}{k_T}\right)^2\right\}^{-1/2}\left\{1+\left(\frac{1}{v}-\frac{\cos\Theta}{v_c}\right)^2\left(\frac{\omega}{k_L}\right)^2\right\}^{-1/2}. \tag{4}$$

The asymptotic behavior of this function for small and for large ω is identical to that of (3), if $k_L^{-1} \sim L$ and $k_T^{-1} \sim \tau$. These relations are fundamental to the following discussions. The statistical models assume that a fault breaks coherently for only short distances, compared to the total fault length, and short times, compared to the total fracture time. The deterministic model (Haskell, 1964) assumes that the dislocation propagates uniformly along the fault. The statistical feature was introduced by Haskell (1966) in order to explain the high-frequency part of observed spectra.

Moment versus Source Area

The concept of seismic moment, introduced into seismology fairly recently, rests on the equivalence between elastic dislocation and a double-force couple (Steketee, 1958; Burridge and Knopoff, 1964; Maruyama, 1963; Aki, 1966; Haskell, 1964). An earthquake fault is mathematically modeled by a shear displacement discontinuity (dislocation) across a surface Σ in an elastic medium. This dislocation is equivalent to a distribution of double couples on this surface whose total moment is

$$M_o = \mu S \bar{D} \tag{5}$$

where μ is the rigidity of the medium, $\bar{D}$ the average dislocation, and S is the area of Σ. The moment of this equivalent double couple is called the seismic moment. Since the dislocation is, in general, a function of time, M_o is also a function of time t. In a restricted usage, the value of M_o at $t \to \infty$ is called the seismic moment. In practice, however, the period at which the determination of M_o is made depends on the kind of available data. Geodetic data give M_o at $t \to \infty$, long-period surface-wave or free oscillation data give M_o at minutes and hours, and body-wave data, at relatively short periods. It is usually assumed that M_o is determined at sufficiently long period so that it represents the value at $t = \infty$. Although this assumption seems reasonable in many cases, it is not necessarily self-evident. It depends, in fact, on the behavior of the spectrum at long periods.

Since long-period waves are less affected by structural complexities than the short-period waves used for the determination of earthquake magnitude, the seismic moment is one of the most reliably determined instrumental earthquake source parameters. For large earthquakes, in particular, the values of M_o determined by different investigators seldom differ by a factor of more than two. For small earthquakes, the uncertainty is usually somewhat larger. Many reliable determinations of seismic slip and moment have been made by using geodetic, surface-wave, free-oscillation, and body-wave data.

The physical dimensions of an earthquake source may be defined by the size of the fault plane or the aftershock area. When the earthquake fault is well defined by field observations or seismic directivity (Ben-Menahem, 1961), the area of the fault plane may be the most unambiguous parameter representing the physical dimension of the source. However, when the source is suboceanic or the earthquake is too small or too deep to break the surface, the fault area cannot be determined directly. In these cases, the size of the aftershock area may be used instead to represent the physical size. Of course, the aftershock area is not a completely unambiguous concept, but it has been shown for several cases that the extent of the aftershock activity immediately after the main shock (hours or days) is consistent with the dimension of the fault length estimated by seismic directivity measurements (Benioff *et al.*, 1961; Ben-Menahem and Toksöz, 1963; Kanamori, 1970a). However, in some cases, particularly for small earthquakes, the

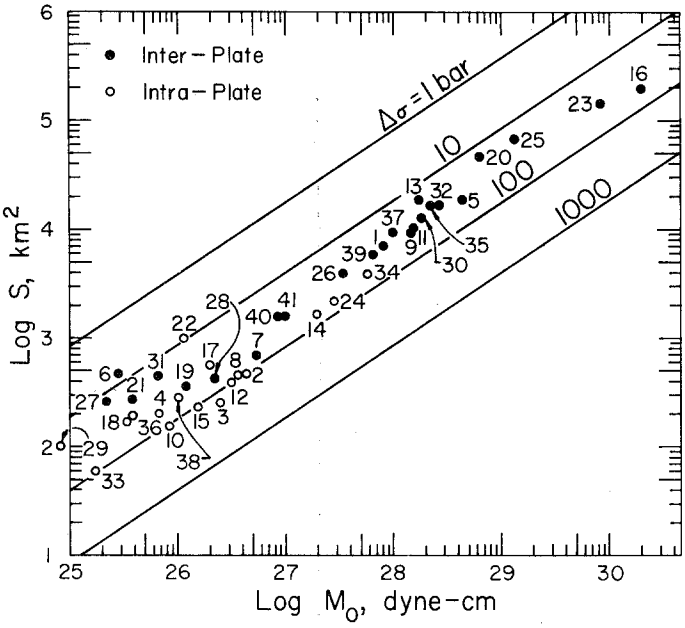

FIG. 2. Relation between S (fault surface area) and M_o (seismic moment). The straight lines give the relations for circular cracks with constant $\Delta\sigma$ (stress drop). The numbers attached to each event correspond to those in Table 1.

aftershock area tends to overestimate the fault area because of the uncertainty in aftershock locations and of the temporal expansion of the aftershock area. In this study, when the fault size is estimated by more than one method, the average is used. Details are given in the references to Table 1 which lists the fundamental earthquake parameters used in this study. A similar table has been published for 34 shallow-focus earthquakes in the Tonga arc by Molnar and Wyss (1972).

The seismic moment and the fault area summarized in Table 1 are plotted in Figure 2. This representation introduced by Aki (1972b) is similar to the one used by Hanks and Thatcher (1972) who used spectral parameters instead of physical parameters. In Figure 2, we classified the earthquakes into two groups, inter-plate and intra-plate earthquakes. The inter-plate earthquakes refer to those which occur along, or parallel to, the major plate boundaries with a large slip rate. Major thrust earthquakes along subduction zones and along transform faults are classed into this group. Earthquakes which occur clearly within the plate are intra-plate earthquakes. In the present paper, earthquakes whose

fault planes are not along the plate boundary are classed as intra-plate earthquakes, even though they occur near the plate boundary. By this definition, the San Fernando and Kern County events are intra-plate earthquakes.

TABLE 1

EARTHQUAKE DATA

No.	Event	Date	M_S	M_o (10^{27} dyne-cm)	S (10^3 km^2)
1	Kanto	Sept. 1, 1923	8.2[5]	8.5[6]	6.9[6]
2	Tango	Mar. 7, 1927	7.75[12]	0.46[11]	0.49[11]
3	N. Izu	Nov. 25, 1930	7.1[1]	0.24[7]	0.24[8]
4	Saitama-1	Sept. 21, 1931	6.75[1]	0.068[9]	0.2[9]
5	Sanriku	Mar. 2, 1933	8.3[10]	43.0[10]	18.5[10]
6	Long Beach	Mar. 11, 1933	6.25[1]	0.028[3]	0.45[12]
7	Imperial Valley	May 19, 1940	7.1[13]	0.56[14]	0.78[14]
8	Tottori	Sept. 10, 1943	7.4[1]	0.36[15]	0.43[15]
9	Tonankai	Dec. 7, 1944	8.2[16]	15[16]	9.6[16]
10	Mikawa	Jan. 12, 1945	7.1[1]	0.087[59]	0.132[59]
11	Nankaido	Dec. 20, 1946	8.2[16]	15[16]	9.6[16]
12	Fukui	Jun. 28, 1948	7.3[1]	0.33[17]	0.39[17]
13	Tokachi-Oki	Mar. 4, 1952	8.3[1]	17[3]	19[18]
14	Kern County	July 21, 1952	7.7[1]	2.0[3]	1.4[19]
15	Fairview Peak	Dec. 16, 1954	7.1[21]	0.15[20]	0.22[20]
16	Chile	May 22, 1960	8.3[21]	2000[22]	200[23]
17	Kitamino	Aug. 19, 1961	7.0[2]	0.21[24]	0.57[24]
18	Wakasa Bay	Mar. 27, 1963	6.9[2]	0.033[25]	0.16[25]
19	N. Atlantic	Aug. 3, 1963	6.7[26]	0.12[26]	0.35[26]
20	Kuril Isl.	Oct. 13, 1963	8.2[21]	67[27]	44[28]
21	N. Atlantic-2	Nov. 17, 1963	6.5[26]	0.038[26]	0.24[26]
22	Spain	Mar. 15, 1964	7.1[33]	0.12[33]	1.0[33]
23	Alaska	Mar. 28, 1964	8.5[21]	820[29]	130[30]
24	Niigata	Jun. 16, 1964	7.4[21]	2.9[31]	2.1[32]
25	Rat Isl.-1	Feb. 4, 1965	7.9[21]	125[34]	78[35]
26	Rat Isl.-2	Mar. 30, 1965	7.5[21]	3.4[36]	4.0[36]
27	Parkfield	Jun 28, 1966	6.4[37]	0.026[38]	0.26[39]
28	Aleutian	July 4, 1966	7.2[26]	0.23[26]	0.42[26]
29	Truckee	Sep. 12, 1966	5.9[57]	0.0083[40]	0.1[40]
30	Peru	Oct. 17, 1966	7.5[41]	20[42]	11.2[42]
31	Borrego Mt.	Apr. 9, 1968	6.7[43]	0.067[44]	0.45[45]
32	Tokachi-Oki	May 16, 1968	8.0[46]	28[47]	15[47]
33	Saitama	July 1, 1968	5.8[48]	0.019[49]	0.06[49]
34	Portuguese	Feb. 28, 1969	8.0[4]	6.0[50]	4.0[50]
35	Kurile Isl.	Aug. 11, 1969	7.8[2]	22.0[51]	15.3[51]
36	Gifu	Sept. 9, 1969	6.6[2]	0.034[52]	0.19[52]
37	Peru	May 31, 1970	7.8[4]	10.0[42]	9.1[42]
38	San Fernando	Feb. 9, 1971	6.6[53]	0.12[54]	0.28[55]
39	Nemuro-Oki	Jun. 16, 1973	7.7[4]	6.7[56]	6.0[56]
40	Turkey	July 22, 1967	7.1[44]	0.83[58]	1.6[58]
41	Iran	Aug. 31, 1968	7.3[4]	1.0[58]	1.6[58]

REFERENCES TO TABLE 1

(1) Gutenberg and Richter (1954)
(2) Usami (1966) or JMA (Japan Meteorological Agency)
(3) Kanamori, unpublished data
(4) USCGS. M_S
(5) (1) and average of 17 stations (Kanamori and Miyamura, 1970)
(6) Average of Kanamori (1971b) and Ando (1971)

REFERENCES TO TABLE 1—*Continued*

(7) Average of (3), Kasahara (1957), and Chinnery (1964)
(8) Average of (3), Kasahara (1957), Chinnery (1964), and Iida (1959)
(9) Abe (1974a)
(10) Kanamori (1971a)
(11) Average of Kanamori (1973) and Kasahara (1957)
(12) (3) and the aftershock area
(13) Richter (1958)
(14) Average of Brune and Allen (1967) and Byerly and DeNoyer (1958)
(15) Kanamori (1972b)
(16) Kanamori (1972a)
(17) Kanamori (1973)
(18) (3) and Utsu and Seki (1954)
(19) (3) and Richter (1955)
(20) Savage and Hastie (1966)
(21) Rothe (1969)
(22) Average of Plafker and Savage (1970), Kanamori and Cipar (1974) and Kanamori and Anderson (1975)
(23) Average of Plafker (1972) and Kanamori and Cipar (1974)
(24) Average of (3) and Kawasaki (1975)
(25) Abe (1974b)
(26) Udias (1971)
(27) Average of Kanamori (1970a) and Ben-Menahem and Rosenman (1972)
(28) Average of Kanamori (1970a), Santo (1964), and Ben-Menahem and Rosenman (1972)
(29) Average of Savage and Hastie (1966), Kanamori (1970b), Abe (1970), Ben-Menahem, Rosenman and Israel (1972), and Alewine and Jungels (1973)
(30) Average of Algermissen *et al.* (1969), Savage and Hastie (1966), and Kanamori (1970b)
(31) Average of Aki (1966), Hirasawa (1965), and Abe (1975b)
(32) Average of Aki (1966), Kayano (1968), Hirasawa (1965), and Abe (1975b)
(33) Udias and Arroyo (1970)
(34) Average of Ben-Menahem and Rosenman (1972) and Wu and Kanamori (1973)
(35) Average of Jordan *et al.* (1965), Ben-Menahem and Rosenman (1972), and Wu and Kanamori (1973)
(36) Abe (1972a)
(37) Wu (1968)
(38) Average of Tsai and Aki (1969), Scholz *et al.* (1969), and Trifunac and Udwadia (1974)
(39) Average of Eaton *et al.* (1970) and Trifunac and Udwadia (1974)
(40) Tsai and Aki (1970)
(41) Average of Pasadena and Berkeley
(42) Abe (1972a)
(43) Average of nine stations
(44) Hanks and Wyss (1972)
(45) Average estimated from surface rupture and aftershock area quoted in Hanks and Wyss (1972)
(46) Average of JMA, Pasadena and Berkeley
(47) Kanamori (1971c)
(48) Average of Abe (1975a) and JMA
(49) Abe (1975b)
(50) Fukao (1973)
(51) Abe (1973)
(52) Average of (3) and Mikumo (1973b)
(53) Average of 39 stations
(54) Average of Wyss (1971), Wyss and Hanks (1972), Canitez and Toksöz (1972), Mikumo (1973a), Savage *et al.* (1975), Jungels and Frazier (1973), Trifunac (1974) and Alewine (1974)
(55) Average of Allen *et al* (1971), Wyss and Hanks (1972), Canitez and Toksöz (1972), Mikumo (1973a), Trifunac (1974), Savage *et al.* (1973) and Whitcomb *et al.* (1973).
(56) Shimazaki (1974)
(57) Average of seven stations
(58) (44), Ambraseys and Zatopek (1969) and Ambraseys and Tchalenko (1969)
(59) Ando (1974)

The most striking feature of Figure 2 is the remarkable linearity with a slope of 2/3 between log S and log M_o. This linearity is usually explained in terms of "constant stress drop". For constant rigidity this implies "constant strain drop." For a circular fault, we have from (1) and (5)

$$M_o = \mu S\bar{D} = \frac{16}{7}\Delta\sigma a^3 = \left(\frac{16\,\Delta\sigma}{7\pi^{3/2}}\right) S^{3/2} \tag{6}$$

or

$$\log M_o = \frac{3}{2}\log S + \log\left(16\,\Delta\sigma/7\pi^{3/2}\right). \tag{7}$$

Thus, for a constant $\Delta\sigma$, $\log S \sim \frac{2}{3}\log M_o$ as shown in Figure 2. For rectangular faults, the constant term depends on the square root of the aspect ratio, w/L. We will use the simplest circular model for the purpose of the present discussion.

Figure 2 shows the relation (7) for four different stress drops. The most remarkable feature is that the large inter-plate earthquakes for which both S and M_o are most accurately (perhaps ± 30 per cent) determined align with a very small scatter between the lines for 10 and 100 bars. A stress drop of 30 bars is indicated for this group of earthquakes. On the other hand, intra-plate earthquakes indicate systematically larger stress drops, about 100 bars. This conclusion is in general agreement with the observation that several intra-plate earthquakes involve higher stresses (Sykes and Sbar, 1973). Molnar and Wyss (1972) found that some events that occur within either the Pacific or Australian plates have higher stress drops than events with the same moment that occur on the boundary of these two plates. If no distinction is made between intra-plate and inter-plate earthquakes, a gross average of 60 bars may be used as a representative value of stress drop for large earthquakes. This stress drop corresponds to a strain drop of $(60\times 10^6)/(3\times 10^{11}) \sim 2\times 10^{-4}$ which agrees, within a factor of two or so, with a value suggested by Tsuboi (1956) for the critical strain of the Earth's crust. Chinnery (1964) and Aki (1972b) concluded, although on relatively few data, that the stress drop in shallow earthquakes is 10 to 100 bars. The more complete data-set presented here substantiates this conclusion.

This type of general relation has also been found for smaller earthquakes by Wyss and Brune (1968), Thatcher and Hanks (1973), and Ishida (1974), but the scatter is much larger, the stress drop ranging from 0.5 to 300 bars. This large scatter may partly represent small scale heterogeneity of the stress field in the crust, but is also due to errors in the dimensions which are determined, in most cases, from the "corner frequency". Since the stress drop is proportional to the cube of the corner period, a small error in the corner period results in a considerable error in the stress drop.

The small scatter in the log S versus log M_o diagram for larger earthquakes strongly indicates that the constant stress-drop model (i.e., constant strain drop, $\bar{D}/\tilde{L}$) is a very good model for large earthquakes.

Magnitude versus Moment

The surface-wave magnitude M_S is determined from the logarithm of the amplitude of surface waves at a period of 20 sec, while the seismic moment M_o is measured, in principle, at infinitely long period. Since surface-wave energy is ultimately derived from

elastic-wave radiation from the source, the dependence of surface-wave amplitude on the spacio-temporal characteristics of the source should be governed by equation (3), or similar relations. Thus, the relation between M_o and M_S can be obtained directly from (3), if we introduce the following similarity conditions

$$\frac{w}{L} = c_1 = \text{const} \qquad \text{(aspect ratio)} \tag{8}$$

$$\frac{\bar{D}}{L} = c_2 = \text{const} \qquad \text{(strain drop)} \tag{9}$$

$$\frac{v\tau}{L} = c_3 = \text{const} \qquad \text{(dynamic similarity)}. \tag{10}$$

(8) represents a geometrical similarity which seems reasonable for most earthquakes. (9) represents constant $\Delta\sigma$ (or strain drop) which is shown, in the preceding section, to be valid for large earthquakes, and (10) represents a dynamic similarity which implies constant effective stress. This last point will be discussed later. With the similarity conditions (8) and (9) the seismic moment $M_o = \mu S\bar{D} \sim L^3$. On the other hand, the magnitude M_S is proportional to $\log |u_c(\omega)|$ at $\omega = \omega_0 = 2\pi/T_0$ ($T_0 = 20$ sec). If we consider the "average azimuth" $\Theta = \pi/2$, then

$$M_S \sim \log \left[\bar{D}Lw \left| \frac{\sin \frac{\omega_0 \tau}{2}}{\frac{\omega_0 \tau}{2}} \right| \left| \frac{\sin \frac{\omega_0}{2} \frac{L}{v}}{\frac{\omega_0}{2} \frac{L}{v}} \right| \right]. \tag{11}$$

The function

$$F\left(\tau, \frac{L}{v}\right) \equiv \left| \frac{\sin \frac{\omega_0 \tau}{2}}{\frac{\omega_0 \tau}{2}} \right| \left| \frac{\sin \frac{\omega_0}{2} \frac{L}{v}}{\frac{\omega_0}{2} \frac{L}{v}} \right|$$

in the above relation takes the following asymptotic values depending on τ and L/v

$$F(\tau, L/v) \sim \begin{cases} \dfrac{vT_0}{\pi L} \sim L^{-1} & \text{if } \tau < \dfrac{T_0}{\pi} \text{ and } \dfrac{L}{v} > \dfrac{T_0}{\pi} \\ \dfrac{1}{\pi} \dfrac{T_0}{\tau} \sim L^{-1} & \text{if } \tau > \dfrac{T_0}{\pi} \text{ and } \dfrac{L}{v} < \dfrac{T_0}{\pi} \\ \dfrac{T_0^2}{\pi^2} \dfrac{v}{L} \dfrac{1}{\tau} \sim L^{-2} & \text{if } \tau > \dfrac{T_0}{\pi} \text{ and } \dfrac{L}{v} > \dfrac{T_0}{\pi} \\ 1 \sim L^0 & \text{if } \tau < \dfrac{T_0}{\pi} \text{ and } \dfrac{L}{v} < \dfrac{T_0}{\pi}. \end{cases}$$

Thus

$$M_S \sim \begin{cases} \log L^2 & \text{if } \tau < \dfrac{T_0}{\pi} \text{ and } \dfrac{L}{v} > \dfrac{T_0}{\pi} \\ \log L^2 & \text{if } \tau > \dfrac{T_0}{\pi} \text{ and } \dfrac{L}{v} < \dfrac{T_0}{\pi} \\ \log L & \text{if } \tau > \dfrac{T_0}{\pi} \text{ and } \dfrac{L}{v} > \dfrac{T_0}{\pi} \\ \log L^3 & \text{if } \tau < \dfrac{T_0}{\pi} \text{ and } \dfrac{L}{v} < \dfrac{T_0}{\pi}. \end{cases}$$

Figure 3 shows the dependence of M_S on L in the four quadrants on $(\tau, L/v)$ plane. Although determinations of the rise time τ are relatively few, available data for about ten

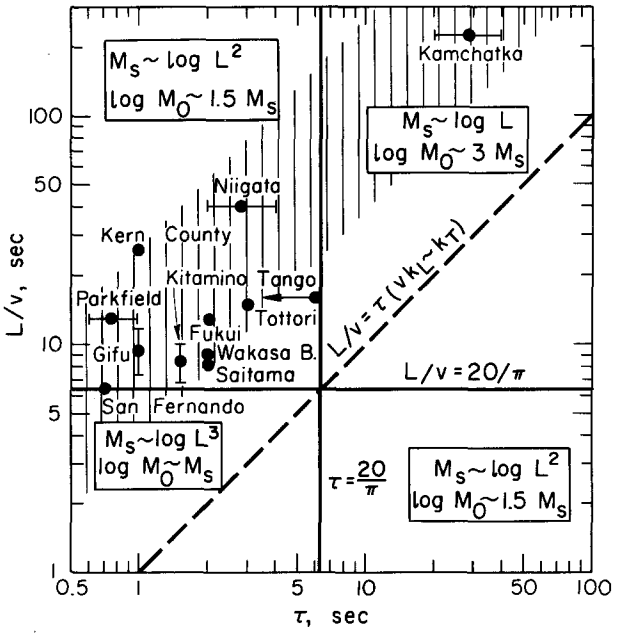

FIG. 3. Relations between rupture time L/v and rise time τ. The dependence of M_S on L and M_o is shown for each quadrant. The earthquake data are taken from the references in Table 1, and Ben-Menahem and Toksöz (1963) for the Kamchatka earthquake.

earthquakes fall mostly within the quadrant for $M_S \sim \log L^2$ as shown in Figure 3. Thus for most large earthquakes for which M_S can be determined, we may put $M_S \sim \log L^2$. Combining this with $M_0 \sim L^3$ we have

$$\log M_0 \sim \frac{3}{2} M_S. \tag{12}$$

The physical interpretation of these results is as follows; $\tau < T_0/\pi$ corresponds to "rapid" rise-time events (< 6 sec). Compared to 20 sec, most seismic events can be considered to have rapid rise times because of the efficiency of generation of 1-sec P waves. Therefore, $M_S \sim \log L^2$ or $\log L^3$ will hold for the majority of events. The term L/v is roughly equivalent to the total time duration of faulting. For reasonable propagation velocities the inequality $L/v > T_0/\pi$ is almost certainly satisfied for $L > 18$ km or $M_S > 6.5$. Therefore, most large earthquakes will satisfy $M_S \sim \log L^2$.

Very small earthquakes with short rise times and small dimension are likely to satisfy $M_S \sim \log L^3$. The conditions $\tau > T_0/\pi$ and $L/v > T_0/\pi$ may be appropriate for slow precursors (Kanamori and Anderson, 1975), tsunami-generating earthquakes of moderate magnitude and mid-Atlantic ridge events which generate large surface waves but small body waves. For large dimension earthquakes with long rise times $M_S \sim \log L$.

We have discussed only surface-wave magnitude but the same arguments hold for body-wave magnitude except that characteristic times are now to be compared with 1 sec rather than 20 sec. In this case, only very small earthquakes can be expected to scale as $m_b \sim \log L^3$ and more earthquakes can be expected to satisfy the $m_b \sim \log L$

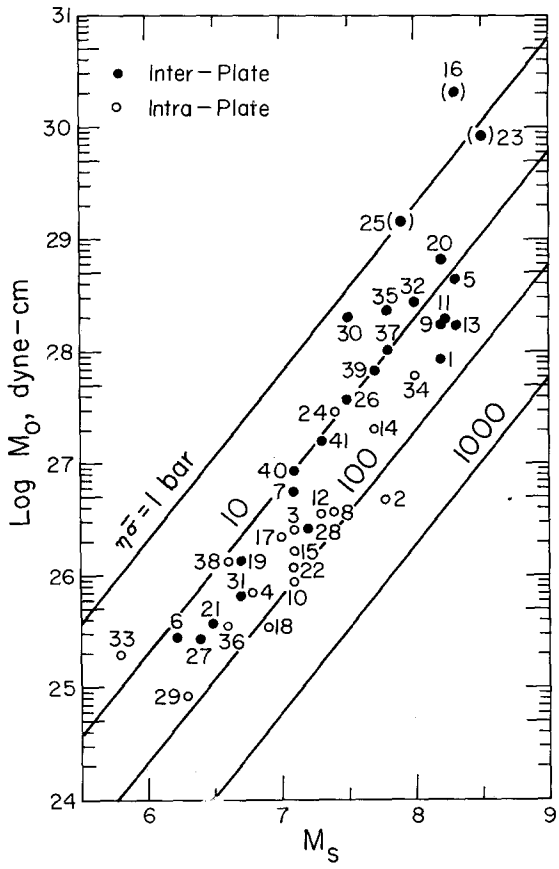

FIG. 4. Relation between M_S (20-sec surface-wave magnitude) and M_o. The straight lines are for constant apparent stress. A rigidity of 3×10^{11} dyne/cm^2 is used.

scaling. However, the validity of the similarity conditions is not very obvious for small earthquakes, and the scaling relations may be more complicated (Aki, 1972a). Since the relation between magnitude and fault length depends on the period of the seismic wave being observed, the $M_S - m_b$ relation will not be linear over a large magnitude range. Most explosions probably satisfy M_S and $m_b \sim \log L^3$ (where L is the cavity radius).

Figure 3 indicates an approximately linear trend between the observed L/v and τ which justifies the dynamic similarity condition (10). Figure 3 also indicates that if the fault length exceeds a certain limit, 100 km or so, then the $M_S \sim \log L^2$ relation (i.e., $\log M_0 \sim 3/2\ M_S$) should be replaced by $M_S \sim \log L$ relation (i.e., $\log M_o \sim 3\ M_S$). Thus for extremely large earthquakes, such as the 1960 Chilean, 1964 Alaskan, and 1965 Rat Island earthquakes, we expect a $\log M_o \sim 3M_S$ relation. Figure 4 shows the relation between

log M_o and M_S for earthquakes listed in Table 1. The slope of 3/2 is indicated by the straight lines in the figure. Although the scatter is considerable, the general trend is consistent with a slope of 3/2 except for very large earthquakes which indicate a much steeper slope corresponding to the log $M_o \sim 3\, M_S$ relation discussed above. Thus, for large earthquakes, the simple dynamic dislocation model with the similarity conditions seems to be an adequate model.

In the above, we used a one-dimensional unilateral rupture. In actual faulting, however, the rupture can be two-dimensional, rectangular (Hirasawa and Stauder, 1965) or circular (Savage, 1966; Sato and Hirasawa, 1973), and bilateral, symmetric or asymmetric, and the critical values of L/v and τ depend on the mode of rupture. For example, for bilateral faultings, L in (11) should be replaced by $L/2$. For circular faults, Sato and Hirasawa (1973) showed (their figure 4) that the critical value of L/v is about T_0/π. These differences in rupture mode, however, would not drastically affect the present conclusion.

Also, we considered the "average azimuth" $\Theta = \pi/2$, but this choice does not affect the present results either. Haskell (1964) integrated

$$R^c_{\theta\phi}\left|\frac{\sin\dfrac{\omega t_c}{2}}{\dfrac{\omega t_c}{2}}\right|$$

over the whole space, and obtained a function $B_2(\omega)$ which is similar to

$$\left(\sin\frac{\omega L}{2v}\Big/\frac{\omega L}{2v}\right)$$

(figure 4 in Haskell, 1964). Using this function leads to about the same critical value of L/v.

The same conclusion may be reached by using Aki's (1967) statistical model with the same similarity conditions. Although the statistical parameters k_L and k_T do not explicitly represent specific physical quantities, it seems reasonable, in view of the similarity conditions, to put ${k_L}^{-1} \sim L$ and ${k_T}^{-1} \sim \tau$. Then, it follows from (4) that

$$M_S \sim \begin{cases} \log L^2 & \text{for } \dfrac{1}{vk_L} > \dfrac{T_0}{2\pi} \text{ and } \dfrac{1}{k_T} < \dfrac{T_0}{2\pi} \\ \log L^2 & \text{for } \dfrac{1}{vk_L} < \dfrac{T_0}{2\pi} \text{ and } \dfrac{1}{k_T} > \dfrac{T_0}{2\pi} \\ \log L & \text{for } \dfrac{1}{vk_L} > \dfrac{T_0}{2\pi} \text{ and } \dfrac{1}{k_T} > \dfrac{T_0}{2\pi} \\ \log L^3 & \text{for } \dfrac{1}{vk_L} < \dfrac{T_0}{2\pi} \text{ and } \dfrac{1}{k_T} < \dfrac{T_0}{2\pi}. \end{cases} \tag{13}$$

Thus for the first two cases we have

$$\log M_o \sim \tfrac{3}{2} M_S.$$

The preceding discussion is analogous to Aki (1967); however, Aki more or less arbitrarily put $vk_L = k_T$ (dotted line in Figure 3), and therefore his scaling law predicts an abrupt transition from log $M_o \sim 3\, M_S$ to log $M_o \sim M_S$ (see figure 4 of Aki, 1972a). As shown in Figure 3, the observed data for τ and L seem to suggest $L/v \sim 10\tau$ or $k_T \sim 10\, vk_L$,

and therefore $\log M_o \sim 3/2\, M_S$ for a considerable range of magnitude. The observed values of M_o and M_S shown in Figure 4 clearly show that this relation holds for large earthquakes. Aki's emphasis is on the overall difference in the spectral characteristics between large and small earthquakes, and replacing $k_T \sim vk_L$ by $k_T \sim 10\, vk_L$ would not significantly affect his conclusions, as Aki (1967) mentioned briefly. Brune and King (1967), Brune (1968), and Brune and Engen (1969) introduced $\log M_o$ versus M_S diagrams which consist of two segments each having a slope of 1. Since they determined the moment at 100-sec period, their relation cannot be directly compared with Figure 4.

The dynamic similarity condition $v\tau/L = \text{const}$ can be given the following physical meaning. The rise time of the dislocation function depends on the effective stress. Brune (1970) showed that the effective stress $\sigma_{e,o}$ (the initial tectonic stress, σ_o, minus the frictional stress, σ_f, opposing the fault motion, i.e., $\sigma_{e,o} = \sigma_o - \sigma_f$) and the dislocation particle velocity $\dot{D}$ are related by

$$\dot{D} = 2\frac{\sigma_{e,o}}{\mu}\beta \tag{14}$$

for infinite rupture velocity. For finite rupture velocity ($v \sim \beta$), it can be shown that (Kanamori, 1972b)

$$\dot{D} \sim \sigma_{e,o}\frac{\beta}{\mu}. \tag{15}$$

Since $\dot{D} \sim \bar{D}/\tau$, and $\bar{D} \sim L$, similarity condition (9), (15) suggests

$$\frac{v\tau}{L} \sim \sigma_{e,o}^{-1}. \tag{16}$$

Thus the dynamic similarity condition is equivalent to constant effective stress. Since determinations of effective stress are very few, the constancy of the effective stress is not so well established as that of the stress drop. However, the data, plotted in Figure 3, showing $v\tau/L \sim$ constant, and a determination of the effective stress in the frequency domain by Trifunac (1972) suggest that the effective stress is, on the average, about constant for large earthquakes. This is reasonable since the effective stress is even more a material property than the stress drop.

Magnitude versus Energy

The relation between the surface-wave magnitude M_S and the total energy of seismic waves E_S has been studied by many investigators, among others, Gutenberg and Richter (1956) and Båth (1958). After several revisions Gutenberg and Richter (1956) obtained a relation

$$\log E_S = 1.5\, M_S + 11.8 \tag{17}$$

(see Richter, 1958, page 366. The constant 11.4 used in this reference is a misprint, and should read 11.8). Båth (1958) integrated the surface wave trains to establish the relation between the surface-wave energy e_s and M_S. Combining this relation with a relation between e_s and the total energy E_S, Båth (1958) finally arrived at a relation

$$\log E_S = 1.44\, M_S + 12.24 \tag{18}$$

which is very similar to (17). M_S represents the level of the energy spectrum at 20 sec while E_S represents the integral of the spectrum over the entire frequency band. Thus,

implicit in (17) or (18) is a certain similarity condition by which the energy spectral density at 20-sec period can represent the whole spectrum, or at least the integral of the spectrum. The above relations (17) and (18) imply that

$$E_S \sim 10^{1.5\,M_S}. \tag{19}$$

This relation, of course, has been introduced empirically, but we shall show in the following that it can be explained in terms of the simple dislocation model we used in the previous section. Using the amplitude spectral density $|u_c(\omega)|$ and the same approximations as we used before, we have

$$E_S \sim \int_0^\infty \omega^2 |u_c{}^2(\omega)|\, d\omega \sim L^2 w^2 D^2 \int_0^\infty \omega^2 \left| \frac{\sin \frac{\omega\tau}{2}}{\frac{\omega\tau}{2}} \right|^2 \left| \frac{\sin \frac{\omega L}{2v}}{\frac{\omega L}{2v}} \right|^2 d\omega$$

$$= \frac{L^2 w^2 D^2}{\tau^3} \Phi\left(\frac{L}{v\tau}\right) \tag{20}$$

where

$$\Phi(x) = \int_0^\infty y^2 \left| \frac{\sin \frac{y}{2}}{\frac{y}{2}} \right|^2 \left| \frac{\sin \frac{xy}{2}}{\sin \frac{xy}{2}} \right|^2 dy. \tag{21}$$

Using the similarity conditions (8), (9) and (10), we have $\Phi(L/v\tau) = \text{const}$ and $L^2 w^2 D^2/\tau^3 \sim L^3$; therefore

$$E_S \sim L^3. \tag{22}$$

Remembering

$$M_S \sim \log L^2 \tag{23}$$

for large earthquakes, we have, from (22)

$$E_S \sim 10^{1.5\,M_S}$$

which is the empirical relation (19). Aki's (1967) statistical model leads to the same since (4) gives

$$E_S \sim \int_0^\infty (w^2 \bar{D}^2 L^2) \frac{\omega^2}{\left(1+\left(\frac{\omega}{vk_L}\right)^2\right)\left(1+\left(\frac{\omega}{k_T}\right)^2\right)} d\omega$$

$$= \frac{\pi}{2} w^2 \bar{D}^2 L^2 (k_T)^2 (k_L v)^2 \frac{1}{k_L v + k_T} \sim L^3$$

where the similarity conditions (8), (9) and (10) are used. Brune's (1970) model also leads to $E_S \sim L^3$ as shown by Hanks and Thatcher (1972).

It is interesting at this point to compare (22) with the energy relation (2) for the static model. The seismic-wave energy E_S may be expressed by

$$E_S = \eta\, \Delta W = \eta S \bar{D} \bar{\sigma} = \frac{\eta}{\mu} M_0 \bar{\sigma} \tag{24}$$

where η is the seismic efficiency. If we use the similarity conditions, $\bar{D} \sim L$, and $S \sim L^2$, we have

$$E_S = \frac{\eta}{\mu} M_o \bar{\sigma} \sim \eta \bar{\sigma} L^3 \tag{25}$$

where $\sigma_a \equiv \eta \bar{\sigma}$ is the apparent stress (Aki, 1966; Wyss, 1970).

Comparison of this with (22) implies that the apparent stress σ_a is constant (i.e., independent of L) for large earthquakes. This is a rather important result which simply arises from the fact that the simple dislocation model together with the similarity conditions predict $E_S \sim L^3$, while a simple static model predicts $E_S \sim \sigma_a L^3$ dependence.

Combining (25) and the Gutenberg-Richter energy relation (17), we have

$$\log M_o = 1.5\, M_S + (11.8 - \log(\sigma_a/\mu)). \tag{26}$$

This relation can be compared with the observed $\log M_o$ versus M_S plot shown by Figure 4. As discussed before, for very large earthquakes with fault lengths exceeding 100 km or so (e.g., Chile, 1960; Alaska, 1964; Rat Island, 1965), this relation is not valid. The data points for these earthquakes are bracketed in Figure 4. Although the scatter is considerable, there is a trend that the intra-plate earthquakes have systematically higher σ_a than inter-plate earthquakes. Very crude estimates would be $\sigma_a \sim 10$ to 20 bars for inter-plate, $\sigma_a \sim 50$ bars for intra-plate, and $\sigma_a \sim 30$ bars for the "average" earthquake. Comparing these values with the values of stress drop $\Delta\sigma$ (Figure 2), we note that $\sigma_a \approx \frac{1}{2}\Delta\sigma$. Although this result involves various uncertainties such as geometry, rigidity, rupture mode, energy-magnitude relation, etc., it is interesting to compare this with the Savage-Wood (1971) inequality

$$\sigma_a < \Delta\sigma/2. \tag{27}$$

This relation results from the fault model of Orowan (1960) and the assumption that the frictional stress σ_f during the slippage is greater than the final stress σ_1. In terms of the average stress $\bar{\sigma}$, frictional stress σ_f and the average dislocation, the efficiency η may be written as

$$\eta = \frac{\bar{\sigma}\bar{D} - \sigma_f \bar{D}}{\bar{\sigma}\bar{D}} = \frac{\bar{\sigma} - \sigma_f}{\bar{\sigma}} \tag{28}$$

or

$$\sigma_f = \bar{\sigma} - \sigma_a. \tag{29}$$

Thus if $\sigma_f > \sigma_1$ we have, from (29),

$$\sigma_a < \tfrac{1}{2}\Delta\sigma$$

which is the Savage-Wood inequality. Our results $\sigma_a \approx \frac{1}{2}\Delta\sigma$ therefore suggests that the final stress is approximately equal to the frictional stress σ_f, i.e., $\sigma_f \sim \sigma_1$. For several earthquakes for which the effective stress $\sigma_{e,o}$ and $\Delta\sigma$ are independently determined, the results indicate $\sigma_{e,o} \sim \Delta\sigma$ (Kanamori, 1972b; Abe, 1974 a,b, 1975a). Since $\sigma_{e,o} = \sigma_o - \sigma_f$ and $\Delta\sigma = \sigma_0 - \sigma_1$, these results indicate $\sigma_f = \sigma_1$ which is consistent with the result obtained above. From (28), σ_f being replaced by σ_1, we have

$$\eta = \frac{\bar{\sigma} - \sigma_1}{\bar{\sigma}} = \frac{\varepsilon}{2 - \varepsilon} \tag{30}$$

where ε is the static fractional stress drop, $\varepsilon = \Delta\sigma/\sigma_0$. By using (30), we can estimate σ_o, and η for intra-plate, inter-plate and "average" earthquakes for various values of

ε (or σ_f/σ_0). The results are shown in Table 2. Since the frictional stress cannot be determined by seismological methods alone, it is not possible to nail down the efficiency and the initial tectonic stress σ_o. The results in Table 2 are interesting, however, in relation to the recently developed dilatancy model of an earthquake. Laboratory experiments on rocks suggest that "kilobar stress" is necessary for the onset of dilatancy. On the other hand, earthquake data invariably suggest 10- to 100-bar stress (either stress drop or apparent stress), which is significantly lower than the laboratory stress. This disparity, however, can be removed, as Table 2 indicates, if a frictional stress is larger than 90 per cent of the tectonic stress; in this case only a part of a "kilobar" tectonic stress is released in earthquakes. Wyss and Molnar (1972) suggested a value of 0.01 to 0.1 for ε for Denver, Colorado, earthquakes.

TABLE 2

FRACTIONAL STRESS DROP (ε), FRACTIONAL FRICTIONAL STRESS σ_f/σ_o, EFFICIENCY (η), INITIAL TECTONIC STRESS (σ_0), STRESS DROP ($\Delta\sigma$) FOR INTER-PLATE, INTRA-PLATE, AND AVERAGE EARTHQUAKES*

ε	$\frac{\sigma_f}{\sigma_o}$	η	σ_o (bar)		
			Inter-plate ($\Delta\sigma=30$ bar)	Intra-plate ($\Delta\sigma=100$ bar)	"Average" ($\Delta\sigma=60$ bar)
1.0	0	1.0	30	100	60
0.8	0.2	0.67	38	125	76
0.6	0.4	0.43	50	170	100
0.4	0.6	0.25	75	250	150
0.2	0.8	0.11	150	500	300
0.1	0.9	0.053	300	1000	600
0.05	0.95	0.026	600	2000	1200
0.01	0.99	0.005	3000	10000	6000

* $\sigma_f/\sigma_0 = 1-\varepsilon$, $\eta = \varepsilon/(2-\varepsilon)$, $\sigma_0 = \Delta\sigma/\varepsilon$.

It should be noted that various assumptions and simplifications have been made in the above discussion. For example, the possible change in gravitational energy associated with earthquake faulting (Jungels and Frazier, 1973) is not considered. Inclusion of this type of energy would affect the energy budget and, therefore, the efficiency. Also, generation of high-frequency energy may not be properly modeled by the simple dislocation model used here. This high-frequency energy is to some extent taken care of by the empirical constant 11.8 in the log E_S versus M_S relation, but detailed discussions are not possible unless more precise estimates of the energy are made in the near-field.

MAGNITUDE VERSUS FAULT AREA

The simple dislocation model, with the similarity conditions, leads to a straightforward relation between M_S and the fault surface area S. For a circular crack, we have from (2) and (24),

$$E_S = \eta\,\Delta W = \frac{16}{7\mu}\,\pi^{-3/2}\,\eta\bar{\sigma}\,\Delta\sigma\,S^{3/2}.$$

Combining this with the log E_S versus M_S relation, and eliminating E_S, we have

$$\log S = M_S + 8.13 - \frac{2}{3}\log\left(\frac{\Delta\sigma}{\mu}\,\sigma_a\right). \tag{31}$$

Thus, if $\Delta\sigma$ and σ_a are constant as we have shown, log S should be proportional to M_S. In fact Utsu and Seki (1954) found a linear relation log $S = 1.02\,M - 4.01$ (S in square kilometers) between the aftershock area and the magnitude (Figure 5). The aftershock area may be considered approximately equal to the fault area. The magnitude scale used by Utsu and Seki (1954) is the JMA (Japan Meteorological Agency) scale which is not the regular surface-wave magnitude M_S, but is calibrated against M_S closely (Tsuboi, 1957). Figure 5 includes the data listed in Table 1 but not used by Utsu and Seki (1954). As shown in Figure 5, the data points for the 1960 Chilean earthquake, the 1964 Alaskan earthquake and the 1965 Rat Island earthquake deviate significantly from the general trend. This deviation is due to the inappropriateness of the E_S versus M_S relation for such large earthquakes with very large fault dimensions. Except for these earthquakes, the

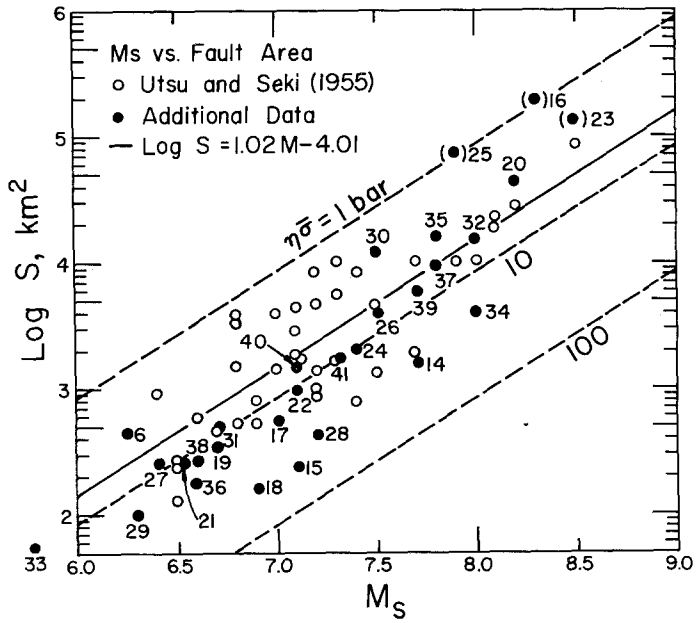

FIG. 5. Relation between M_S and S (aftershock area, fault surface area). The straight lines are for constant apparent stress. The rigidity μ and stress drop of 3×10^{11} dyne/cm^2 and 60 bars are used.

general trend gives a slope of 1.0. If we use $\Delta\sigma = 60$ bars for the "average" earthquakes, σ_a of 2 to 70 bars is consistent with the data. As shown in Figure 5, $\sigma_a = 7$ bars gives a relation which is very close to the Utsu and Seki (1954) relation. In other words, the Gutenberg-Richter relation log $E_S = 1.5\,M_S + 11.8$ and the Utsu-Seki relation log $S = M_S - 4$ (S in square kilometers) suggest $\sigma_a \sim 7$ bars under the assumptions of circular fault, $\mu = 3 \times 10^{11}$ dyne/cm^2 and $\Delta\sigma = 60$ bars. The relatively large scatter in the M_S versus log S diagram is partly due to the ambiguity in the aftershock area. Utsu and Seki (1954) did not clearly define it, but they seem to have taken the area which includes all of the aftershocks during a considerably long period of time after the main shock. The aftershock area thus defined tends to overestimate the fault size. Nevertheless, it is notable that this independent set of data suggests σ_a of 2 to 70 bars in general agreement with the value estimated from the log M_o versus M_S relation, about 30 bars. Båth and Duda (1964) suggest a somewhat different relation

$$\log S = 1.21\,M_S - 5.05 \qquad (S \text{ in square kilometers})$$

which is in general agreement with Utsu and Seki (1954).

Tsuboi (1956) assumed that the total energy of an earthquake E is given by $E = \frac{1}{2}ex^2V$ where e is the effective elastic constant, x is the ultimate strain and V the "earthquake volume". Using this energy in the log E_S versus M_S relation, Tsuboi derived the Utsu and Seki (1954) relation. Implicit in his derivation are, in terms of the present model, the assumptions of complete stress drop (in the relation $E = \frac{1}{2}ex^2V$) and 100 percent efficiency ($\eta = 1.0$). Thus Tsuboi's model is a special case of the present model. He used $x = 10^{-4}$ which corresponds to $\Delta\sigma = \mu x = 30$ bars. The assumption of complete stress drop and $\eta = 1$ gives $\eta\bar{\sigma} = \frac{1}{2}\Delta\sigma$. Putting these into (31), we have $\log S = M_S - 4.0$ (S in square kilometers) which is essentially the Utsu and Seki (1954) relation.

Magnitude versus Frequency

The magnitude-frequency relation is given by

$$\log N = a - bM_S \tag{32}$$

where N is the number of earthquakes in a certain magnitude range $M_S \pm \frac{1}{2}\Delta M_S$, or the number of earthquakes larger than M_S, in a certain area, and a and b are constants. Except for some volcanic events, the value of b has been found to be very close to 1. This result can be explained in terms of a simple geometrical consideration. Consider an area Σ, and let $N(M_S)$ and $S(M_S)$ be the number and the fault area of earthquakes within a magnitude range around M_S in this area. Since the smaller the $S(M_S)$, the more faults can be accommodated in Σ, it seems reasonable to put

$$N(M_S)S(M_S) \sim \Sigma = \text{const.} \tag{33}$$

Then

$$\log N \sim -\log S.$$

Combining this with (31), we have

$$\log N \sim M_S. \tag{34}$$

Thus the observation that the b value in the magnitude-frequency relation is close to 1 can be explained by a geometrical relation given by (33). It is important to note that the relation $S \sim 10^{M_S}$ we used above came from $E_s \sim 10^{1.5\,M_S}$ to which we gave a physical explanation on the basis of the simple dislocation model.

The recurrence time of an earthquake of magnitude M is proportional to N^{-1}, thus $\tau \sim N^{-1} \sim S \sim L^2$. This implies that if the rate of various processes associated with earthquakes, such as strain rate, etc., is uniform, other times such as various precursor times scale the same. The $\tau \sim L^2$ relation does not imply diffusion.

Discussion

We have determined the following theoretical relationships,

$$\log M_o = 1.5 \log S + \log \Delta\sigma + \log C$$

where

$$\begin{aligned} C &= 16/7\pi^{3/2} \quad \text{(circular faults)} \\ &= (\pi/2)(w/L)^{1/2} \quad \text{(strike slip)} \\ &= \pi(\lambda+2\mu)(w/L)^{1/2}/4(\lambda+\mu) \quad \text{(dip slip).} \end{aligned}$$

The seismic data are consistent with this relation and imply stress drops, $\Delta\sigma$, of 30 and 100 bars, respectively, for inter-plate and intra-plate earthquakes.

Radiated elastic energy, E_S, is

$$E_S = \frac{M_o}{\mu}\eta\bar{\sigma}.$$

Therefore $\log E_S = \log M_o + \log(\eta\bar{\sigma}/\mu) = 1.5 \log S + \log \Delta\sigma + \log(\eta\bar{\sigma}) + \log C$.

The apparent stress, $\sigma_a = \eta\bar{\sigma}$, is 10 to 20 bars and 50 bars, respectively, for inter-plate and intra-plate earthquakes. Therefore $\eta\bar{\sigma} \sim \Delta\sigma/2$.

By assuming geometric and dynamic similarity we obtain

$$M_S = \log(\bar{D}L^n w) + b = \log \tilde{L}^{n+2} + b'$$

where

$n = +1, 0, -1$ depending on the ordering of the characteristic times, τ and t_c, and the measurement period T_o ($\sim$ 20 sec for M_S and $\sim$ 1 sec for m_b);

$M_S \sim \log \tilde{L}^2 \sim (2/3) \log M_o \sim (2/3) \log E_S$ (most moderate to large earthquakes)

$M_S \sim \log \tilde{L} \sim (1/3) \log M_o \sim (1/3) \log E_S$ (long rise time large events)

$M_S \sim \log \tilde{L}^3 \sim \log M_o \sim \log E_S$ (very small earthquakes).

The relation

$$\log E_S \sim 1.5\, M_S$$

is the Gutenberg-Richter relation and is appropriate for most events. However, $\log E_S \sim 3M_S$ and $\log E_S \sim M_S$ hold for the special cases noted above.

The geometric similarity condition $w \sim L$ may break down for large earthquakes if there is a maximum depth over which brittle fracture occurs. This may hold for large transform-fault events where $w < 20$ km regardless of the length. In this case, $w \sim$ const and, from $\Delta\sigma \sim \bar{D}/w = $ const, $\bar{D} \sim$ const. Therefore $\tau \sim \bar{D}/v = $ const, and, from (11), $M_S \sim L^0$. Thus the magnitude does not depend on fault length although the moment, $M_o = \mu\, \bar{D} w L \sim L$, does.

Conclusion

An extensive data-set of the seismic moment M_o and the fault surface area, S, for large earthquakes ($M_S \geq 6$) demonstrates a remarkably linear relation between $\log S$ and $\log M_o$ with a slope of 2/3 indicating a constant stress drop, $\Delta\sigma$, for large earthquakes. $\Delta\sigma = 30$, 100 and 60 bars are suggested for inter-plate, intra-plate and "average" earthquakes, respectively. Except for very large earthquakes, the relation $\log M_o \sim 1.5\, M_S$ (20-sec surface-wave magnitude) is established by the data for large earthquakes. This relation can be explained in terms of a spectral shape of seismic radiation predicted by a very simple dislocation model such as Haskell's (1964). This dislocation model predicts a relation $\log E_S \sim 1.5\, M_S$ (E_S, the total radiated wave energy) consistent with the empirical M_S versus E_S relation of Gutenberg and Richter (1956) and Båth (1958). The model also predicts $E_S \sim L^3$ (L, the representative fault dimension) which in turn suggests a constant apparent stress since the static energy is also proportional to L^3. An apparent stress about half the stress drop is suggested. These relations lead to $\log S \sim M_S$ consistent with the empirical relation suggested by Utsu and Seki (1954).

The magnitude-frequency relation $\log N(M_S) \sim -M_S$ ($N(M_S)$ is the number of

earthquakes in magnitude range around M_S) can then be interpreted in terms of a simple geometrical model $N(M_S) \cdot S(M_S) =$ constant where $S(M_S)$ is the fault surface area.

Although the values of the stress implied by seismic data are low, 10 to 100 bars, it is possible that the tectonic stress is very high ($\sim$ kilobars) and that only a small fraction of it is released in earthquakes, the frictional stress being high.

Acknowledgments

We thank Tom Hanks and Bob Geller for useful discussions.

This research was supported by the Advanced Research Projects Agency of the Department of Defense and was monitored by the Air Force Office of Scientific Research under Contract F44620-72-C-0078, and Earth Sciences Section of the National Science Foundation under Grant DES74-22489.

References

Abe, K. (1970). Determination of seismic moment and energy from the earth's free oscillation, *Phys. Earth Planet. Interiors* **4**, 49–61.

Abe, K. (1972a). Lithospheric normal faulting beneath the Aleutian trench, *Phys. Earth Planet. Interiors* **5** 190–198.

Abe, K. (1972b). Mechanisms and tectonic implications of the 1966 and 1970 Peru earthquakes, *Phys. Earth Planet. Interiors* **5**, 367–379.

Abe, K. (1973). Tsunami and mechanism of great earthquakes, *Phys. Earth Planet. Interiors* **7**, 143–153.

Abe, K. (1974a). Seismic displacement and ground motion near a fault: The Saitama earthquake of September 21, 1931, *J. Geophys. Res.* **79**, 4393–4399.

Abe, K. (1974b). Fault parameters determined by near- and far-field data: The Wakasa Bay earthquake of March 26, 1963, *Bull. Seism. Soc. Am.* **64**, 1369–1382.

Abe, K. (1975a). Static and dynamic parameters of the Saitama earthquake of July 1, 1968, *Tectonophysics* (in press).

Abe, K. (1975b). A fault model for the Niigata earthquake of 1964, *J. Phys. Earth.* (in press).

Aki, K. (1966). Generation and propagation of *G* waves from the Niigata earthquake of June 16, 1964, *Bull. Earthquake Res. Inst., Tokyo Univ.* **44**, 23–88.

Aki, K. (1967). Scaling law of seismic spectrum, *J. Geophys. Res.* **72**, 1217–1231.

Aki, K. (1972a). Scaling law of earthquake source time-function, *Geophys. J.* **31** 3–25.

Aki, K. (1972b). Earthquake mechanism, *Tectonophysics* **13**, 423–446.

Alewine, R. W. III (1974). Application of linear inversion theory toward the estimation of seismic source parameters, *Thesis*, California Institute of Technology, Pasadena, California.

Alewine, R. W. III and P. H. Jungels (1973). Application of stochastic inversion theory and the finite-element method to zero-frequency seismology: The 1964 Alaska earthquake, *Caltech Preprint.*

Algermissen, S. T., W. A. Rinehart, R. W. Sherburne, and W. H. Dillinger, Jr. (1969). Preshocks and aftershocks of the Prince William Sound earthquake of March 28, 1964, in *The Prince William Sound, Alaska earthquake of 1964 and aftershocks*, Vol. 2, L. E. Leipold, Editor, pp. 79–130, U.S. Department of Commerce, Environmental Science Services Administration, Washington, D.C.

Allen, C. R., G. R. Engen, T. C. Hanks, J. M. Nordquist, and W. R. Thatcher (1971). Main shock and larger aftershocks of the San Fernando earthquake, February 9 through March 1, 1971, *U.S. Geol. Surv. Profess. Paper 733*, 17–20.

Ambraseys, N. N. and J. S. Tchalenko (1969). The Dasht-e-Bayaz (Iran) earthquake of August 31, 1968: A field report, *Bull. Seism. Soc. Am.* **59**, 1751–1792.

Ambraseys, N. N. and A. Zatopek (1969). The Mudurnu Valley, West Anatolia, Turkey, earthquake of July 22, 1967, *Bull. Seism. Soc. Am.* **59**, 521–589.

Ando, M. (1971). A fault-origin model of the great Kanto earthquake of 1923 as deduced from geodetic data, *Bull. Earthquake Res. Inst., Tokyo Univ.* **49**, 19–32.

Ando, M. (1974). Faulting in the Mikawa earthquake of 1945, *Tectonophysics* **22**, 173–186.

Båth, M. (1958). The energies of seismic body waves and surface waves, in *Contributions in Geophysics: In Honor of Beno Gutenberg*, H. Benioff, M. Ewing, B. F. Howell, Jr., and F. Press, Editors, Pergamon Press, New York, pp. 1–16.

Båth, M. and S. J. Duda, (1964). Earthquake volume, fault plane area, seismic energy, strain, deformation and related quantities, *Ann. Geofis. (Rome)* **17**, 353–368.

Ben-Menahem, A. (1961). Radiation of seismic surface waves from finite moving sources, *Bull. Seism. Soc. Am.* **51,** 401–435.

Ben-Menahem, A. and M. Rosenman (1972). Amplitude patterns of Tsunami waves from submarine earthquakes, *J. Geophys. Res.* **77,** 3097–3128.

Ben-Menahem, A., M. Rosenman, and M. Israel (1972). Source mechanism of the Alaskan earthquake of 1964 from amplitudes of free oscillations and surface waves, *Phys. Earth Planet. Interiors* **5,** 1–29.

Ben-Menahem, A. and M. N. Toksöz (1963). Source mechanism from spectrums of long-period surface waves, *J. Geophys. Res.* **68,** 5207–5222.

Benioff, H., F. Press, and S. W. Smith (1961). Excitation of the free oscillations of the earth by earthquakes, *J. Geophys. Res.* **66,** 605–619.

Brune, J. (1968). Seismic moment, seismicity and rate of slip along major fault zones, *J. Geophys. Res.* **73,** 777–784.

Brune, J. (1970). Tectonic strain and the spectra of seismic shear waves from earthquakes, *J. Geophys. Res.* **75,** 4997–5009.

Brune, J. N. and C. R. Allen (1967). A low-stress-drop, low-magnitude earthquake with surface faulting: The Imperial, California, earthquake of March 4, 1966, *Bull. Seism. Soc. Am.* **57,** 501–514.

Brune, J. N. and G. R. Engen (1969). Excitation of mantle Love waves and definition of mantle wave magnitude, *Bull. Seism. Soc. Am.* **59,** 923–933.

Brune, J. N. and C. Y. King (1967). Excitation of mantle Rayleigh waves of period 100 seconds as a function of magnitude, *Bull. Seism. Soc. Am.* **57,** 1355–1365.

Burridge, R. and L. Knopoff (1964). Body force equivalents for seismic dislocations, *Bull. Seism. Soc. Am.* **54,** 1875–1888.

Byerly, P. and J. De Noyer (1958). Energy in earthquakes as computed for geodetic observations, in *Contributions in Geophysics, In Honor of Beno Gutenberg*, H. Benioff, M. Ewing, B. F. Howell and F. Press, Editors, Pergamon Press, New York, pp. 17–35.

Canitez, N. and M. N. Toksöz (1972). Static and dynamic study of earthquake source mechanism: San Fernando earthquake, *J. Geophys. Res.* **77,** 2583–2594.

Chinnery, M. A. (1964). The strength of the earth's crust under horizontal shear stress, *J. Geophys. Res.* **69,** 2085–2089.

Eaton, J. P., M. E. O'Neill, and J. N. Murdock (1970). Aftershocks of the 1966 Parkfield-Cholame, California earthquake: A detailed study, *Bull. Seism. Soc. Am.* **60,** 1151–1197.

Eshelby, J. D. (1957). The determination of the elastic field of an ellipsoidal inclusion and related problems, *Proc. Roy. Soc. London, Series A,* **241,** 376–396.

Fukao, Y. (1973). Thrust faulting at a lithospheric plate boundary. The Portugal earthquake of 1969, *Earth Planet. Sci. Letters* **18,** 205–216.

Gutenberg, B. and C. F. Richter (1954). *Seismicity of the Earth*, Princeton Univ. Press, Princeton, pp. 310.

Gutenberg, B. and C. F. Richter (1956). Earthquake magnitude, intensity, energy and acceleration, *Bull. Seism. Soc. Am.* **46,** 105–145.

Hanks, T. C. and W. Thatcher (1972). A graphical representation of seismic source parameters, *J. Geophys. Res.* **23,** 4393–4405.

Hanks, T. C. and M. Wyss (1972). The use of body-wave spectra in the determination of seismic-source parameters, *Bull. Seism. Soc. Am.* **62,** 561–589.

Haskell, N. (1964). Total energy and energy spectral density of elastic wave radiation from propagating faults, *Bull. Seism. Soc. Am.* **56,** 1811–1842.

Haskell, N. (1966). Total energy and energy spectral density of elastic wave radiation from propagating faults, 2, *Bull. Seism. Soc. Am.* **56,** 125–140.

Hirasawa, T. (1965). Source mechanism of the Niigata earthquake of June 16, 1964, as derived from body waves, *J. Phys. Earth* **13,** 35–66.

Hirasawa, T. and W. Stauder (1965). On the seismic body waves from a finite moving source, *Bull. Seism. Soc. Am.* **55,** 237–262.

Iida, K. (1959). Earthquake energy and earthquake fault, *J. Earth. Sci., Nagoya Univ.* **7,** 98–107.

Ishida, M. (1974). Determination of fault parameters of small earthquakes in the Kii peninsula, *J. Phys. Earth* **22,** 177–212.

Jordan, J. N., J. F. Lander, and R. A. Black (1965). Aftershocks of the 4 February 1965 Rat Island earthquake, *Science* **148,** 1323–1325.

Jungels, P. H. and G. A. Frazier (1973). Finite element analysis of the residual displacements for an earthquake rupture: Source parameters for the San Fernando earthquake, *J. Geophys. Res.* **78,** 5062–5083.

Kanamori, H. (1970a). Synthesis of long-period surface waves and its application to earthquake source studies—Kurile Islands earthquake of October 13, 1963, *J. Geophys. Res.* **75,** 5011–5027.

Kanamori, H. (1970b). The Alaska earthquake of 1964: Radiation of long-period surface waves and source mechanism, *J. Geophys. Res.* **75**, 5029–5040.

Kanamori, H. (1971a). Seismological evidence for a lithospheric normal faulting—The Sanriku earthquake of 1933, *Phys. Earth Planet. Interiors* **4**, 289–300.

Kanamori, H. (1971b). Faulting of the great Kanto earthquake of 1923 as revealed by seismological data, *Bull. Earthquake Res. Inst., Tokyo Univ.* **49**, 13–18.

Kanamori, H. (1971c). Focal mechanism of the Tokachi-Oki earthquake of May 16, 1968: Contortion of the lithosphere at a junction of two trenches, *Tectonophysics* **12**, 1–13.

Kanamori, H. (1972a). Tectonic implications of the 1944 Tonanki and the 1946 Nankaido earthquakes, *Phys. Earth Planet. Interiors* **5**, 129–139.

Kanamori, H. (1972b). Determination of effective tectonic stress associated with earthquake faulting—Tottori earthquake of 1943, *Phys. Earth Planet. Interiors* **5**, 426–434.

Kanamori, H. (1973). Mode of strain release associated with major earthquakes in Japan, *Ann. Rev. Earth and Planet. Sci.* **1**, 213–239.

Kanamori, H. and D. L. Anderson (1975). Amplitude of the earth's free oscillations and long-period characteristics of the earthquake source, *J. Geophys. Res.* **80**, 1075–1078.

Kanamori, H. and J. J. Cipar (1974). Focal process of the great Chilean earthquake May 22, 1960, *Phys. Earth Planet. Interiors* **9**, 128–136.

Kanamori, H. and S. Miyamura (1970). Seismometrical re-evaluation of the great Kanto earthquake of September 1, 1923, *Bull. Earthquake Res. Inst., Tokyo Univ.* **48**, 115–125.

Kasahara, K. (1957). The nature of seismic origins as inferred from seismological and geodetic observations, 1, *Bull. Earthquake Res. Inst., Tokyo Univ.* **35**, 473–532.

Kawasaki, I. (1975). The focal process of the Kita-Mino earthquake of August 19, 1961, and its relationship to a quaternary fault. The Hatogayu-Koike fault *J. Phys. Earth* (in press).

Kayano, I. (1968). Determination of origin times, epicenters and focal depths of aftershocks of the Niigata earthquake of June 16, 1964, *Bull. Earthquake Res. Inst., Tokyo Univ.* **46**, 223–269.

Keilis, Borok, V. (1959). On estimation of the displacement in an earthquake source and of source dimensions, *Ann. Geofis. (Rome)* **12**, 205–214.

Knopoff, L. (1958). Energy release in earthquakes, *Geophys. J.* **1**, 44–52.

Maruyama, T. (1963). On the force equivalents of dynamic elastic dislocations with reference to the earthquake mechanism, *Bull. Earthquake Res. Inst., Tokyo Univ.* **41**, 467–486.

Mikumo, T. (1973a). Faulting process of the San Fernando earthquake of February 9, 1971 inferred from static and dynamic near-field displacements, *Bull. Seism. Soc. Am.* **63**, 249–269.

Mikumo, T. (1973b). Faulting mechanism of the Gifu earthquake of September 9, 1969, and some related problems, *J. Phys. Earth* **21**, 191–212.

Molnar, P. and M. Wyss (1972). Moments, source dimensions and stress drops of shallow-focus earthquakes in the Tonga-Kermadec arc, *Phys. Earth Planet. Interiors* **6**, 263–278.

Orowan, E. (1960). Mechanism of seismic faulting, *Geol. Soc. Am. Mem.* **79**, 323–345.

Plafker, G. (1972). Alaskan earthquake of 1964 and Chilean earthquake of 1960: Implications for arc tectonics, *J. Geophys. Res.* **77**, 901–925.

Plafker, G. and J. C. Savage (1970). Mechanism of the Chilean earthquakes of May 21 and 22, 1960, *Bull. Geol. Soc. Am.* **81**, 1001–1030.

Richter, C. F. (1955). *Foreshocks and aftershocks, in earthquakes in Kern County, California, during 1952, Part 2 Seismology*, California Division of Mines, 177–197.

Richter, C. F. (1958). *Elementary Seismology*, W. H. Freeman, San Francisco, 768 pp.

Rothe, J. P. (1969). *The Seismicity of the Earth*, UNESCO 336.

Santo, T. (1964). Shock sequences of the southern Kurile Islands from October 9 to December 31, 1963, *Bull. Intern. Inst. Seism. Earthquake Eng.* **1**, 33.

Sato, R. (1972). Stress drop for a finite fault, *J. Phys. Earth* **20**, 397–407.

Sato, T. and T. Hirasawa (1973). Body was spectra from propagating shear cracks, *J. Phys. Earth* **21**, 415–431.

Savage, J. C. (1966). Radiation from a realistic model of faulting, *Bull. Seism. Soc. Am.* **56**, 577–592.

Savage, J. C., R. O. Burford, and W. T. Kinoshita (1975). Earth movements from geodetic measurements, *Calif. Div. Mines and Geol. Bull.* **196**, 175–186.

Savage, J. C. and L. M. Hastie (1966). Surface deformation associated with dip-slip faulting, *J. Geophys. Res.* **71**, 4897–4904.

Savage, J. C. and M. D. Wood (1971). The relation between apparent stress and stress drop, *Bull. Seism. Soc. Am.* **61**, 1381–1388.

Scholz, C. H., M. Wyss, and S. W. Smith (1969). Seismic and aseismic slip on the San Andreas fault, *J. Geophys. Res.* **74**, 2049–2069.

Shimazaki, K. (1974). Nemuro-Oki earthquake of June 17, 1973: A lithospheric rebound at the upper half of the interface, *Phys. Earth Planet. Interiors* **9,** 314–327.

Starr, A. T. (1928). Slip in a crystal and rupture in a solid due to shear, *Proc. Cambridge Phil. Soc.* **24,** 489–500.

Steketee, J. A. (1958). Volterra's dislocations in a semi-infinite medium, *Can. J. Phys.* **36,** 192–205.

Sykes, L. R. and M. L. Sbar (1973). Intraplate earthquakes, lithospheric stresses and the driving mechanism of plate tectonics, *Nature* **245,** 298–302.

Thatcher, W. and T. Hanks (1973). Source parameters of southern California earthquakes, *J. Geophys. Res.* **78,** 8547–8576.

Trifunac, M. D. (1972). Stress estimates for the San Fernando, California earthquake of February 9, 1971; Main event and thirteen aftershocks, *Bull. Seism. Soc. Am.* **62,** 721–750.

Trifunac, M. D. (1974). A three-dimensional dislocation model for the San Fernando, California earthquake of February 9, 1971, *Bull. Seism. Soc. Am.* **64,** 149–172.

Trifunac, M. D. and F. G. Udwadia (1974). Parkfield, California, earthquake of June 27, 1966: A three-dimensional moving dislocation, *Bull. Seism. Soc. Am.* **64,** 511–533.

Tsai, Y. B. and K. Aki (1969). Simultaneous determination of the seismic moment and attenuation of seismic surface waves, *Bull. Seism. Soc. Am.* **59,** 275–287.

Tsai, Y. B. and K. Aki (1970). Source mechanism of the Truckee, California, earthquake of September 12, 1966, *Bull. Seism. Soc. Am.* **60,** 1199–1208.

Tsuboi, C. (1956). Earthquake energy, earthquake volume, aftershock area and strength of the earth's crust, *J. Phys. Earth* **4,** 63–66.

Tsuboi, C. (1957). Energy accounts of earthquakes in and near Japan, *J. Phys. Earth* **5,** 1–7.

Udias, A. (1971). Source parameters of earthquakes from spectra of Rayleigh waves, *Geophys. J.* **22,** 353–376.

Udias, A. and A. L. Arroyo (1970). Body and surface wave study of source parameters of the March 15, 1964 Spanish earthquake, *Tectonophysics* **9,** 323–346.

Usami, T. (1966). Descriptive table of major earthquakes in and near Japan which were accompanied by damages, *Bull. Earthquake Res. Inst., Tokyo Univ.* **44,** 1571–1622.

Utsu, T. and A. Seki (1954). A relation between the area of aftershock region and the energy of main shock, *J. Seism. Soc. Japan* **7,** 233–240.

Whitcomb, J. H., C. R. Allen, J. D. Garmany and J. A. Hileman (1973). San Fernando earthquake series, 1971: Focal mechanisms and tectonics, *Rev. Geophys. Space Phys.* **11,** 693–730.

Wu, F. T. (1968). Parkfield earthquake of June 28, 1966: Magnitude and source mechanism, *Bull. Seism. Soc. Am.* **58,** 689–709.

Wu, F. T. and H. Kanamori (1973). Source mechanism of February 4, 1965, Rat Island earthquake, *J. Geophys. Res.* **78,** 6082–6092.

Wyss, M. (1970). Stress estimates of South American shallow and deep earthquakes, *J. Geophys. Res.* **75,** 1529–1544.

Wyss, M. (1971). Preliminary source parameter determination of the San Fernando earthquake, *U.S. Geol. Surv. Profess. Paper 733,* 38–40, Washington, D.C.

Wyss, M. and P. Molnar (1972). Efficiency, stress drop, apparent stress, effective stress and frictional stress of Denver, Colorado, earthquakes, *J. Geophys. Res.* **77,** 1433–1438.

Wyss, M. and J. N. Brune (1968). Seismic moment, stress and source dimensions for earthquakes in the California-Nevada region, *J. Geophys. Res.* **73,** 4681–4694.

Wyss, M. and T. C. Hanks (1972). The source parameters of the San Fernando earthquake inferred from teleseismic body waves, *Bull. Seism. Soc. Am.* **62,** 591–602.

SEISMOLOGICAL LABORATORY
DIVISION OF GEOLOGICAL AND PLANETARY SCIENCES
CALIFORNIA INSTITUTE OF TECHNOLOGY
PASADENA, CALIFORNIA 91125
CONTRIBUTION NO. 2612.

Manuscript received April 8, 1975